

Reading molecular messages from the intersections of high-order harmonic spectra at different orientation angles

Y. J. Chen^{1,2}, J. Liu^{2,3*}, and Bambi Hu^{1,4}

1. *Department of Physics, Centre for Nonlinear Studies,
and The Beijing-Hong Kong-Singapore Joint Centre for Nonlinear and Complex Systems (Hong Kong),
Hong Kong Baptist University, Kowloon Tong, Hong Kong, China*

2. *Institute of Applied Physics and Computational Mathematics, Beijing 100088, China*

3. *Center for Applied Physics and Technology, Peking University, Beijing 100084, China*

4. *Department of Physics, University of Houston, Houston, Texas 77204-5005.*

(Dated: October 26, 2018)

We investigate the orientation dependence of high-order harmonic generation (HHG) from H_2^+ with different internuclear distances irradiated by intense laser fields both numerically and analytically. The calculated molecular HHG spectra are found to be sensitive to molecular axis orientation relative to incident laser field polarization and internuclear separation. In particular, the spectra calculated for different orientation angles demonstrate a kind of intersection, which is identified as arising due to intramolecular two-center interference in the HHG. The striking "intersection" phenomenon can be used to probe the molecular instantaneous structure.

PACS numbers: 33.80.Rv, 42.65.Ky, 32.80.Rm

High-order harmonic generation (HHG) from aligned molecules in strong laser fields of femtosecond duration has proven to be a powerful tool for resolving and controlling the processes in an ultrafast time scale. For instance, recent experiments showed that calibrating the molecular recollision electronic wave packet by a reference atom, the HHG spectra can be used to image molecular orbital[1], and measuring the interference minima in the HHG spectra[2, 3, 4, 5], the HHG can also be used to probe molecular instantaneous structure[6, 7]. Moreover, the investigations on the molecular orbital tomography[8, 9, 10, 11, 12] and the effects of two-center interference in the HHG[13, 14, 15, 16, 17, 18, 19] are leading valuable insights into the mechanism of atomic and molecular HHG.

Nevertheless, theoretical studies demonstrated that in some cases, the molecular properties already enter the recollision electronic wave packet. Accordingly, the spectral amplitude of the molecular recollision electronic wave packet is largely different from its reference atom in some energy regions[20]. This implies that accurately calibrating the molecular recollision electronic wave packet can be difficult for some species of molecules. In addition, it was revealed that both two-center interference[2] and the interference between different recombination electron trajectories[21] are responsible for the suppressed harmonics at certain orders. As a result, the minima in harmonic spectra may shift as the laser intensity changes[22].

In the present paper, numerically investigating the orientation dependence of the HHG from H_2^+ with different internuclear distances, we find that the molecular HHG spectra are sensitive to molecular axis orientation relative to incident laser field polarization as well as to the internuclear separation. In particular, the spectra calculated for different orientation angles demonstrate a kind of intersection, which is identified as arising due to intramolecular two-center interference in the HHG. Com-

pared to the interference-related minima in the HHG spectra, the intersections of the harmonic spectra are easy to identify in practice. This finding is advocated for promising applications as a prospective tool to probe the molecular structure and dynamics.

Let us consider the Hamiltonian of H_2^+ as (the atom units of $\hbar = e = m_e = 1$ are used throughout this paper)

$$H(t) = \mathbf{p}^2/2 + V(\mathbf{r}) - \mathbf{r} \cdot \mathbf{E}(t), \quad (1)$$

where $V(\mathbf{r})$ is the Coulomb potential and $\mathbf{E}(t)$ is the external electric field. In the 2D case, the Coulomb potential is written as $V(x, y) = \frac{-Z}{\sqrt{0.5+(x+R/2)^2+y^2}} + \frac{-Z}{\sqrt{0.5+(x-R/2)^2+y^2}}$, where Z is the effective charge, and R is the internuclear separation, (for $Z = 1$ and $R = 2$ a.u., the ground state energy for H_2^+ reproduced here is $I_p = 1.11$ a.u.). In this paper, we assume that the molecular axis is coincident with the x-axis and the external field $\mathbf{E}(t) = E\vec{e}\sin(\omega_0 t)$ is linearly polarized with an orientation angle of θ to the molecular axis. E and ω_0 are the amplitude and angular frequency of the laser field. \vec{e} is the unit vector along the laser polarization. Our calculation will be considered for 780 nm trapezoidally shaped laser pulses with a total duration of 10 optical cycles and linear ramps of three optical cycles. Numerically, the Schrödinger equation with the above Hamiltonian $H(t)$ is solved by the operator-splitting method with 2048 time steps per optical cycle. The numerical convergence is checked using a finer grid. The coherent part of the harmonic spectrum is obtained from the Fourier transformed dipole acceleration expectation value, and only the harmonics polarized parallel to the incoming field are considered[2].

To analytically investigate the molecular HHG, we use the Lewenstein model[21] and consider the acceleration effect of the bound potential[1, 2]. The time-dependent

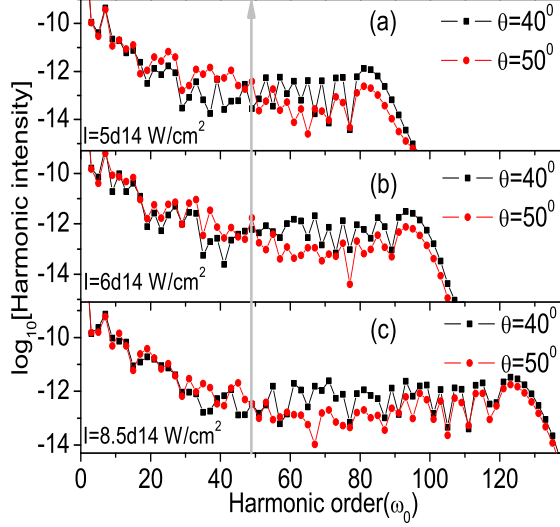


Figure 1: Harmonic spectra of 2D H_2^+ with $Z = 1$, $R = 2$ a.u. at different laser intensities and orientation angles θ , obtained by the exact numerical calculation.

dipole moment is given by[15, 16]

$$\mathbf{x}(t) = i \int_0^\infty d\tau \left(\frac{\pi}{\epsilon + i\tau/2} \right) \mathbf{d}_{rec}^* (\mathbf{p}_{st} - \mathbf{A}(t)) e^{-iS(p_{st}, t, \tau)} \times \mathbf{E}(t - \tau) \cdot \mathbf{d}_{ion} (\mathbf{p}_{st} - \mathbf{A}(t - \tau)) + c.c., \quad (2)$$

where $S(p_{st}, t, \tau) = \int_{t-\tau}^t dt'' [(\mathbf{p}_{st} - \mathbf{A}(t''))^2 / 2 + I_p]$ is the semiclassical action, $\mathbf{A}(t) = -\int \mathbf{E}(t') dt'$ is the vector potential of the external field, and $\mathbf{p}_{st} = \int_{t-\tau}^t dt'' \mathbf{A}(t'') / \tau$ is the canonical momentum corresponding to the stationary value. $\mathbf{d}_{ion}(\mathbf{p}) = \langle \mathbf{p} | \hat{\mathbf{r}} | 0 \rangle = (2\pi)^{-3/2} \int_{-\infty}^\infty d\mathbf{r} \exp(-\mathbf{p} \cdot \mathbf{r}) \mathbf{r} | \mathbf{r} \rangle$ is the bound-free dipole transition matrix element between the molecular ground state $|0\rangle$ and the continuum $|\mathbf{p}\rangle$ in the ionization step, and $\mathbf{d}_{rec}(\mathbf{p}) = \langle \mathbf{p}_k | \hat{\mathbf{r}} | 0 \rangle = (2\pi)^{-3/2} \int_{-\infty}^\infty d\mathbf{r} \exp(-\mathbf{p}_k \cdot \mathbf{r}) \mathbf{r} | \mathbf{r} \rangle$ is that in the recombination step which considers the effect of the electron acceleration in the vicinity of the parent ion before recombination, i.e., the effective momentum $\mathbf{p}_k = \sqrt{\mathbf{p}^2 + 2I_p} \mathbf{p} / |\mathbf{p}|$ is adopted to describe the acceleration effect[1, 2, 9, 15].

The wave function of the valence orbital of the H_2^+ molecule with $1s\sigma_g$ symmetry, investigated here, is expressed in the LCAO-MO approximation

$$\psi_{1s\sigma_g}(\mathbf{r}) = N_{1s\sigma_g} [\phi_{1s}(\mathbf{r} + \mathbf{R}/2) + \phi_{1s}(\mathbf{r} - \mathbf{R}/2)], \quad (3)$$

where N_{1s} is the normalization factor, ϕ_{1s} is the atomic $1s$ orbital in the configuration space, and \mathbf{R} is the vector between the two atomic cores of the molecule. Then, the dipole transition moment for H_2^+ can be written as

$$\mathbf{d}_{1s\sigma_g}(\mathbf{p}) = 2i N_{1s\sigma_g}' [-\cos(\mathbf{p} \cdot \mathbf{R}/2) \mathbf{d}_{1s}(\mathbf{p}) + \sin(\mathbf{p} \cdot \mathbf{R}/2) \tilde{\phi}_{1s}(\mathbf{p}) \mathbf{R}/2], \quad (4)$$

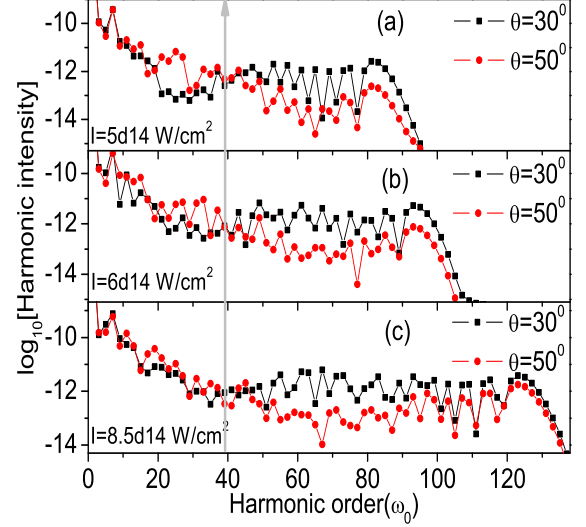


Figure 2: Harmonic spectra of 2D H_2^+ with $Z = 1$, $R = 2$ a.u. at different laser intensities and orientation angles θ , obtained by the exact numerical calculation.

where $\mathbf{d}_{1s}(\mathbf{p})$ is the atomic dipole moment from the $1s$ orbital, and $\tilde{\phi}_{1s}(\mathbf{p})$ is the $1s$ wave function in the momentum space.

In Eq. 4, The factor $\cos(\mathbf{p} \cdot \mathbf{R}/2)$ represents two-center interference[23], and the term, which is proportional to the internuclear distance R , leads to the breakdown of translation invariance. In our calculations, this term is omitted according to Ref.[24, 25, 26]. Then, we obtain

$$\mathbf{d}_{1s\sigma_g}^{mod}(\mathbf{p}) = N_{1s\sigma_g} [-2i \cos(\mathbf{p} \cdot \mathbf{R}/2) \mathbf{d}_{1s}(\mathbf{p})]. \quad (5)$$

In Fig. 1, we plot the harmonic spectra of 2D H_2^+ with $Z = 1$, $R = 2$ a.u. at different laser intensities and orientation angles θ , obtained by the exact numerical calculation. The comparison between the black and red curves in each subpanel of Fig. 1 shows that the harmonic spectra have a broad region within the HHG plateau with highly suppressed harmonic emission rate. The center of the suppressed region shifts to higher harmonic order as the orientation angle θ increases. The broad suppressed regions arise from the two-center interference effect in the molecular HHG[2, 20]. But the locations of the minima in the broad suppressed regions are difficult to identify in some cases. For example, for $\theta = 50^\circ$, in Fig. 1(c), the minimum is clear at the 67th order. Fig. 1(b) is not as clear as Fig. 1(c).

It has been revealed in Ref.[22] that the interference minima in the molecular HHG spectra may shift as the laser intensity changes. In particular, according to the simple point-emitter model proposed in Ref[3], for H_2^+ with $R = 2$ a.u. and $\theta = 50^\circ$, the predicted interference minimum is at the 51st order. Compared to the observation of the 67th order in Fig. 1(c), a large shift of about

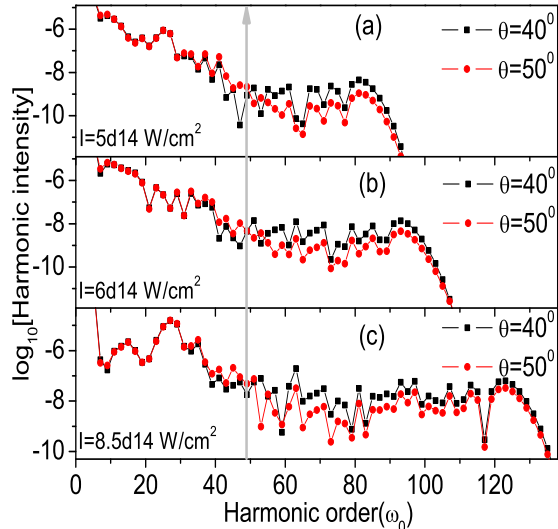


Figure 3: Harmonic spectra of 2D H_2^+ with $Z = 1$, $R = 2$ a.u. at different laser intensities and orientation angles θ , calculated using the Lewenstein model.

16 orders occurs here. Based on the above analyses and discussions, we expect that probing molecular structure using the pronounced interference-related minimum can not be applicable in some cases.

However, as we can see in each subpanel of Fig. 1, the two harmonic spectra at different orientation angles θ demonstrate an intersection in the plateau region. For example, in Fig. 1(c), the black curve for $\theta = 40^\circ$ is lower from the 19th to the 49th order, while the red curve for $\theta = 50^\circ$ is lower from the 49th to the 93rd order. The striking intersection of the two curves is at the 49th order. As the laser intensity changes, the intersection of the two curves is almost invariable, as indicated by the vertical solid line. The calculated harmonic spectra at other orientation angles θ also show the similar phenomena as those revealed in Fig. 1. But the intersections of the harmonic curves change as the orientation angles change. For example, as presented in Fig. 2, the intersection of two harmonic curves at $\theta = 30^\circ$ and $\theta = 50^\circ$ is at the 39th order (indicated by the vertical solid line). This is different from that in Fig. 1.

Next, we concentrate on the physical mechanism behind these phenomena. In Fig. 3, with the same parameters as in Fig. 1, we plot the harmonic spectra calculated using the Lewenstein model Eq. 2 and the modified transition dipole Eq. 5. One can see that the primary characteristics of the harmonic spectra in Fig. 3 are analogous with those of the corresponding curves in Fig. 1. For instance, in each subpanel of Fig. 3, the intersection of two harmonic spectra in the plateau region is at the 49th order, as indicated by the vertical solid curves. This is in agreement with that in Fig. 1. The parallelism between

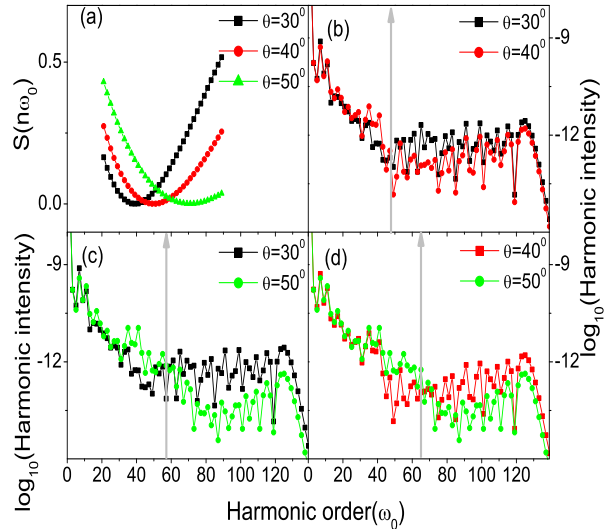


Figure 4: Function curves of $S(n\omega_0)$ and harmonic spectra of 2D H_2^+ with $Z = 1$, $R = 1.7$ a.u. at different orientation angles θ . (a): Function curves; (b), (c) and (d): harmonic spectra obtained by the exact numerical calculation. The laser intensity used here is $I = 8.5 \times 10^{14} \text{W/cm}^2$.

the corresponding curves in Fig. 1 and Fig. 3 shows that the modified model, i.e., Eq. 2 with Eq. 5, is applicable here for the description of the molecular HHG, especially for the angle dependence of the HHG. This applicability is also consolidated below.

From the expressions of Eq. 2 and Eq. 5, we conjecture that the effects of two-center interference are responsible for the intersections of the harmonic spectra at different orientation angles. This conjecture is verified by the following analyses. According to Ref.[1, 9], the harmonic intensity $F(\Omega = n\omega_0, \theta)$ along the laser polarization can be written as $F(\Omega, \theta) \propto \Omega^4 |a(\Omega, \theta) D(\mathbf{p}, \theta)|^2$, where $a(\Omega, \theta)$ is the spectral amplitude of the molecular recollision electronic wave packet, $D(\mathbf{p}, \theta) = \vec{e} \cdot \mathbf{d}_{1s\sigma_g}^{mod}(\mathbf{p})$, and $\Omega = E_{\mathbf{p}} + I_p$ [27]. $E_{\mathbf{p}}$ is the electronic kinetic energy. The spectral amplitude $a(\Omega, \theta)$ is closely related to the ionization process[8, 21]. The transition dipole $D(\mathbf{p}, \theta)$ corresponds to the recombination process. Both $a(\Omega, \theta)$ and $D(\mathbf{p}, \theta)$ are alignment dependent[20]. Here, we focus on $D(\mathbf{p}, \theta)$. The angle θ in the expression of $D(\mathbf{p}, \theta)$ is contained in the cos function in Eq. 5. We extract the cos function from $D(\mathbf{p}, \theta)$, and write its power as

$$S(n\omega_0) = \cos(pR/2 \cos \theta) \cos(pR/2 \cos \theta), \quad (6)$$

with the dispersion relation $n\omega_0 = p^2/2$, that considers the electron acceleration before recombination[1]. n is the harmonic order.

Based on the results shown in Fig. 3, we expect that Eq. 6 gives a good description of the orientation dependence of the HHG from H_2^+ . In Fig. 4 and Fig. 5,

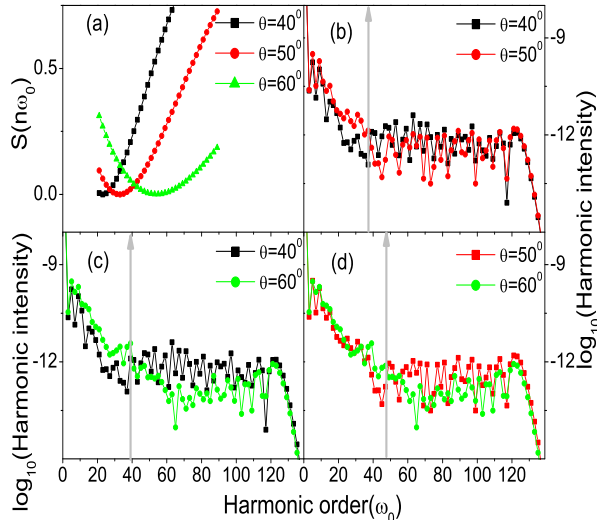


Figure 5: Function curves of $S(n\omega_0)$ and harmonic spectra of 2D H_2^+ with $Z = 1$, $R = 2.5$ a.u. at different orientation angles θ . (a): Function curves; (b), (c) and (d): harmonic spectra obtained by the exact numerical calculation. The laser intensity used here is $I = 8.5 \times 10^{14} \text{ W/cm}^2$.

we show the comparisons between the function curves of Eq. 6 and the corresponding harmonic spectra at varied orientation angles θ and internuclear distances R . These comparisons demonstrate the applicability of Eq. 6 in the prediction of the intersection of two harmonic spectra at different orientation angles θ .

Specifically, for $R = 1.7$ a.u., in Fig. 4(a), the formula predicts that the intersections of two harmonic spectra are at the 45th order for $\theta = 30^\circ$ and $\theta = 40^\circ$, the 53rd order for $\theta = 30^\circ$ and $\theta = 50^\circ$, and the 61st order for $\theta = 40^\circ$ and $\theta = 50^\circ$. In the numerical cases in Fig. 4(b)-(d), the corresponding intersections are at the 47th order, the 57th order and the 65th order, respectively. For $R = 2.5$ a.u., in Fig. 5(a), the formula predicts that those are at the 29th order for $\theta = 40^\circ$ and $\theta = 50^\circ$, the 35th order for $\theta = 40^\circ$ and $\theta = 60^\circ$, and the 43rd order for $\theta = 50^\circ$ and $\theta = 60^\circ$. In Fig. 5(b)-(d), the corresponding intersections are at the 37th order, the 39th order and the 47th order, respectively. The large difference in the case of $\theta = 40^\circ$ and $\theta = 50^\circ$, is due to the breakdown of the dispersion relation, used in our simulation, in the low energy region[28, 29]. For $R = 2$ a.u., the formula also gives a good prediction.

In addition, one can see from Fig. 4 and Fig. 5 that, the interference-related minima are not distinct in the harmonic spectra. It should be mentioned that our numerical method and obtained HHG spectra are comparable to the previous work of Ref.[2, 3, 4]. However, in con-

trary to the claim of Ref.[2, 3, 4], we find that the broad suppressed regions in the harmonic spectra arise from the effects of two-center interference in the HHG, while the locations of the interference-related minima in the HHG spectra predicted in Ref.[2, 3, 4] are difficult to identify, as shown above. Notice that in Ref.[3, 4], a spectrum-smoothing procedure is used to help the identification of the interference minima. This procedure is not adopted in our analysis, since we think it somehow ambiguous and we expect a "direct" comparison of the numerical observations to the experimental measurements.

There are two factors those could influence the position of the interference minimum. First, two-center interference occurs not only in the recombination process of the HHG, but also in the ionization process of the HHG (into intermediate continuum states). The interference factor $\cos(\mathbf{P} \cdot \mathbf{R}/2)$ is also included in the transition dipole $\mathbf{d}_{ion}(\mathbf{p})$ in Eq. 2 that corresponds to the ionization process. As a result, the spectral amplitude $a(\Omega, \theta)$ of the molecular recollision electronic wave packet, which is responsible for the fine structure of the molecular HHG spectrum, may be affected by the interference[20]. Secondly, besides the ground state, the first excited state can also contribute to the harmonic emission in the broad suppressed region of the molecular HHG spectrum[30]. Accordingly, the interference pattern may be modulated by the population of the first excited state.

However, the parallelism between the predictions of Eq. 6 and the numerical results, as discussed above, reveals that the intersections of the HHG spectra could be less influenced by the two factors. Particularly, compared to the interference-related minima, the intersections are easier to identify. These suggest that we can measure the molecular bond length through the measurement of harmonic spectra at different orientation angles θ , using the following equation

$$S(n_s \omega_0, \theta_1) = S(n_s \omega_0, \theta_2), \quad (7)$$

where n_s is the harmonic order that corresponds to the intersection of two harmonic spectra at the orientation angles θ_1 and θ_2 .

In conclusion, we have shown that due to the effects of two-center interference in the HHG, the harmonic spectra of H_2^+ at different orientation angles demonstrate the striking intersections in the high-frequency plateau region. The phenomena discussed here are general. They are expected to appear in other species of molecules. Our results can be useful for promising applications allowing to use the "intersection" phenomenon as a prospective tool to probe the molecular structure and dynamics.

This work is supported in part by Hong Kong Baptist University and the Hong Kong Research Grants Council, and NNSF(No.10725521), 973 research program No.2006CB921400, 2007CB814800.

-
- [*] Liu_Jie@iapcm.ac.cn
- [1] J. Itatani, J. Levesque, D. Zeidler, Hiromichi Niikura, H. Pepin, J. C. Kieffer, P. B. Corkum, and D. M. Villeneuve, *Nature* **432**, 867(2004).
- [2] M. Lein, N. Hay, R. Velotta, J. P. Marangos, and P. L. Knight, *Phys. Rev. Lett* **88**, 183903, (2002).
- [3] M. Lein, N. Hay, R. Velotta, J. P. Marangos, and P. L. Knight, *Phys. Rev. A* **66**, 023805 (2002).
- [4] M. Lein, P. P. Corso, J. P. Marangos, and P. L. Knight, *Phys. Rev. A* **67**, 023819 (2003).
- [5] G. Lagmago Kamta and A. D. Bandrauk, *Phys. Rev. A* **71**, 053407 (2005).
- [6] T. Kanai, S. Minemoto, and H. Sakai, *Nature* **435**, 470(2005).
- [7] C. Vozzi, F. Calegari, E. Benedetti, J.-P. Caumes, G. Sansone, S. Stagira, M. Nisoli, R. Torres, E. Heesel, N. Kajumba, J. P. Marangos, C. Altucci, and R. Velotta, *Phys. Rev. Lett.* **95**, 153902 (2005).
- [8] J. Itatani, D. Zeidler, J. Levesque, Michael Spanner, D. M. Villeneuve, and P. B. Corkum, *Phys. Rev. Lett* **94**, 123902, (2005).
- [9] J. Levesque, D. Zeidler, J. P. Marangos, P. B. Corkum, and D. M. Villeneuve, *Phys. Rev. Lett.* **98**, 183903 (2007).
- [10] S. Patchkovskii, Z. Zhao, T. Brabec, and D. M. Villeneuve, *Phys. Rev. Lett* **97**, 123004, (2006).
- [11] R. Torres, N. Kajumba, Jonathan G. Underwood, J. S. Robinson, S. Baker, J.W. G. Tisch, R. de Nalda, W. A. Bryan, R. Velotta, C. Altucci, I. C. E. Turcu, and J. P. Marangos, *Phys. Rev. Lett* **98**, 203007, (2007).
- [12] Van-Hoang Le, Anh-Thu Le, Rui-Hua Xie, and C. D. Lin, *Phys. Rev. A* **76**, 013414 (2007)
- [13] Anh-Thu Le, X. M. Tong, and C. D. Lin, *Phys. Rev. A* **73** 041402(R) (2006).
- [14] C. Figueira de Morisson Faria, *Phys. Rev. A* **76**, 043407(2007).
- [15] T. Kanai, S. Minemoto, and H. Sakai, *Phys. Rev. Lett.* **98**, 053002 (2007).
- [16] M. F. Ciappina, C. C. Chirilă and M. Lein, *Phys. Rev. A* **75**, 043405 (2007).
- [17] N. Wagner *et al.*, *Phys. Rev. A* **76**, 061403(R) (2007).
- [18] M. F. Ciappina, A. Becker and A. Jaroń-Becker, *Phys. Rev. A* **76**, 063406 (2007).
- [19] V. I. Usachenko, P. E. Pyak, and S. I. Chu, *Laser Phys.* **16**, 1326 (2006).
- [20] Y. Chen, Y. Li, S. Yang, and J. Liu, *Phys. Rev. A* **77**, 031402(R) (2008).
- [21] M. Lewenstein, Ph. Balcou, M. Yu. Ivanov, Anne L’Huillier, and P. B. Corkum, *Phys. Rev. A* **49**, 2117(1994).
- [22] Y. J. Chen and J. Liu, *Phys. Rev. A* **77**, 013410 (2008).
- [23] J. Muth-Böhm, A. Becker, and F. H. M. Faisal, *Phys. Rev. Lett.* **85**, 2280(4) (2000)
- [24] J. Chen and S. G. Chen, *Phys. Rev. A* **75**, 041402(R) (2007).
- [25] D. B. Milosevic, *Phys. Rev. A* **74**, 063404 (2006).
- [26] W. Becker, J. Chen, S. G. Chen, and D. B. Milosevic, *Phys. Rev. A* **76**, 033403 (2007).
- [27] P. B. Corkum, *Phys. Rev. Lett.* **71**, 1994(1993).
- [28] Zhangjin Chen, Toru Morishita, Anh-Thu Le, M. Wickenhauer, X. M. Tong, and C. D. Lin, *Phys. Rev. A* **74** 053405 (2006).
- [29] Xibin Zhou, Robynne Lock, Wen Li, Nick Wagner, Margaret M. Murnane, and Henry C. Kapteyn, *Phys. Rev. Lett.* **100**, 073902 (2008).
- [30] Y. J. Chen, J. Liu, and Bambi Hu, High-order Harmonic Generation in a Time-integrated Quantum Transition Picture, unpublished.